Korean J. Chem. Eng., **30**(4), 898-905 (2013)
DOI: 10.1007/s11814-012-0180-3

The removal of perchlorate using amine-functionalized mesoporous anion-exchange resins with different number of ligands

Byunghwan Lee*,†, Sang Don Lee*, and Kwang-Ho Choo**

*Department of Chemical System Engineering, Keimyung University, 1095, Dalgubeoldaero, Dalseo-gu, Daegu 704-701, Korea
**Department of Environmental Engineering, Kyungpook National University,
1370, Sankyeok-dong, Buk-gu, Daegu 702-701, Korea
(*Received 31 July 2012 • accepted 17 October 2012*)

Abstract−Perchlorate anion (ClO_4^-) in water has become an environmental issue because it can impair proper functioning of the thyroid gland. For the removal of perchlorate anions from water, adsorption using anion-exchange resins has been generally used as the most suitable method. We have prepared mesoporous anion-exchange resins via simple functionalization of amine ligands with different numbers of functional groups, and used them for the removal of perchlorate anions from aqueous solutions. The physical and chemical properties of the prepared samples were measured using nitrogen adsorption-desorption measurement, elemental analyses, X-ray diffraction, and Fourier transform infrared spectroscopy. We also investigated equilibrium isotherms for the measurement of adsorption capacities and kinetic performances of the prepared samples. The prepared materials showed fast adsorption kinetic performances, and M-3N among the prepared materials exhibited high perchlorate adsorption capacity of 175.4 mg/g compared with the results of the previous reports.

Key words: Perchlorate, Mesoporous Materials, Amine Ligands, Anion-exchange Resin

INTRODUCTION

Recently perchlorate anion (ClO_4^-) in water has become an environmental issue because it can impair proper functioning of the thyroid gland [1,2]. Perchlorate is very soluble in water, kinetically inert to reduction, and has little tendency to adsorb to mineral or organic surfaces. Therefore, the anion persists in water, and the mobility in surface or groundwater is very high, finally resulting in the concentration in organisms. Compounds containing perchlorate include the oxidant in solid rocket fuel or fireworks, military ordinance, flares, airbags, and other applications where an energetic oxidant is required. Perchlorate contamination is a national problem with significant concentrations being found in 26 states in the U.S. and Puerto Rico [2]. A very high concentration of perchlorate of 2.23 ppm, which was as 91 times as the USEPA's maximum contaminant level (24.5 ppb), was also reported in Nakdong river, Korea [3].

Biological process or physical adsorption process has been generally adopted to remove the perchlorate anions from aqueous solutions [4]. Among methods used, adsorption using anion-exchange resins has been one of the most suitable methods for the treatment of perchlorate anions of low concentrations [4-10]. However, organic anion-exchange resins, which are used in the adsorption process, have some drawbacks such as thermal/chemical instability, low surface area, hydrophobicity of polymer matrix, and swelling or deformation in contact with solvents. To overcome these drawbacks, organic/inorganic hybrid anion-exchange resins have been synthesized and widely used to remove anions from wastewater [11-13].

Since the development of mesoporous materials [14-16], various adsorbents based on the mesoporous materials have been used for the adsorption of metal ions and organic pollutants by the incorporation of the functional ligands onto the mesoporous materials [17]. Some mesoporous silica materials have been used as supports of the organic/inorganic hybrid anion-exchange resins because they have high density of silanol groups (0.5-3.0/nm^2) [18] and good mass transfer characteristics due to the uniform pore structures. For instance, amine-functionalized mesoporous materials [18], mesoporous materials containing metals, metal cations, or metal oxides [19-23], and mesoporous alumina [24] have been prepared and used for the separation of arsenate, chromate, phosphate, or cesium from aqueous solutions. Mesoporous silicas, organosilica-based mesoporous materials, and bead-type mesoporous materials, which were functionalized with quaternary ammonium groups, have been also successfully synthesized and used to remove perchlorate or perrhenate anions from aqueous solutions [11,12,25-28].

Among the functionalized mesoporous materials, amine ligand-incorporated mesoporous materials have been applied for various purposes including anion adsorption [18], cation adsorption [19,29], CO_2 sorption [30,31], catalyst [32], drug delivery [33], etc. Amine-functionalized mesoporous materials have been generally used for the adsorption of cations in water [19,29]. However, the positively charged surface amino groups, which are obtained via simple acid treatment of the surface, could interact with arsenate ($HAsO_4^{2-}$) or chromate (CrO_4^{2-}) anions, which have two negative charges, in the aqueous solution [18]. To our knowledge, no systematic investigations have been carried out using amine ligand-functionalized mesoporous materials with different numbers of functional groups for the removal of perchlorate (ClO_4^-) anions, which have a negative charge, from aqueous solutions. We prepared two types of meso-

†To whom correspondence should be addressed.
E-mail: leeb@kmu.ac.kr

porous anion-exchange resins (MCM-41 type and SBA-15 type) containing different numbers of amine ligands (1N, 2N, and 3N), and used them for the removal of perchlorate anions from aqueous solutions.

MATERIALS AND METHODS

1. Reagents

The following were used as received without further purification: cetyltrimethylammonium bromide (CTAB, 95%, Aldrich), ammonium hydroxide solution (NH_4OH, 28.0-30.0%, Aldrich), tetraethyl orthosilicate (TEOS, 98%, Aldrich), poly(ethylene glycol)-block-poly(propylene glycol)-block-poly(ethylene glycol) (Pluronic P-123, $EO_{20}PO_{70}EO_{20}$, Aldrich), hydrochloric acid (HCl, 37%, Aldrich), 3-aminopropyltrimethoxysilane (1N, 99%, Aldrich), [1-(2-aminoethyl)-3-amino-propyl]trimethoxysilane (2N, 97%, Aldrich), (trimethoxysilyl)propyldiethylenetriamine (3N, tech, Acros), toluene (99.5% Duksan), 2-propanol (99.5%, Daejung), and sodium perchlorate ($NaClO_4$, ≥98.0%, Aldrich).

2. Syntheses and Characterizations

MCM-41[32,34]: CTAB of 2.97 g was dissolved in 40 ml of distilled water at 50 °C. Then 8.99 ml of NH_4OH and 7.28 ml of TEOS was slowly added to the solution, and the mixture was then stirred for 24 h. The final molar composition of reactants was 1 CTAB : 500 H_2O : 1.8 NH_4OH : 7.5 TEOS. The filtered solid was washed with a large amount of distilled water. The resulting powders were dried in oven at 120 °C for 3 h and in vacuum at 150 °C for another 5 h, and then calcined for 3 h at 550 °C to remove the templates.

SBA-15 [32,35]: P-123 of 2 g was dissolved in the mixture of 15 ml of water and 50 ml of 2 M HCl at 45 °C. To this mixture, 4.25 g of TEOS was added, stirred for 20 h at 45 °C, and then aged at 85 °C for 12 h. The filtered silica materials were vacuum-dried overnight at room temperature, and then calcined for 6 h at 550 °C to remove the templates. The final molar composition of reactants was 0.017 P-123 : 202.6 H_2O : 2.9 HCl : 1 TEOS.

Amine-functionalized mesoporous anion-exchange resin [18]: To prepare MCM-41 functionalized with mono-amine ligands (M-1N), MCM-41 materials prepared were first dehydrated for 4 h at 150 °C in a vacuum to remove water molecules adsorbed on the surface. The solids of 1 g were then stirred vigorously in 100 ml of toluene containing 0.9 ml of 1 N ligand. The mixture was heated to 110 °C in dry nitrogen for 6 h. The filtered powder was washed with 2-propanol for 2 h, and dried at 100 °C for 4 h. Then, 0.1 g of the powder was stirred in 100 mL of 0.1 M HCl for 6 h without heating. This process converted amino groups into ammonium salts, and then M-1N was obtained. MCM-41 materials functionalized with di-amine ligands (M-2N) and tri-amine ligands (M-3N) were also prepared via the similar procedure using 2N and 3N ligands, respectively. SBA-15 materials functionalized with mono-amine ligands (S-1N), di-amine ligands (S-2N), and tri-amine ligands (S-3N) were also prepared via similar procedures using SBA-15 as a support host instead of MCM-41.

Characterizations: N_2 adsorption/desorption measurements (ASAP 2010, Micromeritics, USA) were performed at 77 K. The surface areas of the prepared samples were determined by BET method, and the pore size distribution was obtained from BJH adsorption data. X-ray diffraction (XRD) patterns were obtained at 40 kV and 25 mA using CuK_α radiation (wavelength=0.154 nm) on a powder X-ray diffractometer (X'pert APD, Philips). Fourier transform infrared (FTIR, Research2, ATI Mattson, US) spectroscopy was used to examine the existence of organic groups in the prepared samples. A CHNS corder (Flash 2000, ThermoFisher) was used to measure the amount of functional groups in the samples.

3. Anion Adsorption

Adsorption isotherms were obtained via batch equilibrium experiments. Anion-exchange resin of 0.1 g was mixed with 10 ml of aqueous solutions containing perchlorates, of which concentrations ranged from 25 mg/*l* to 3,600 mg/*l*. The mixtures were sonicated at 45 W for 10 min using an ultrasonic machine (KODO, JAC-1505), stirred at room temperature for 6 h, and then filtered using 0.45 μm membrane. The concentration of perchlorate was measured by ion chromatography (IC, Dionex, DX-120) equipped with an IonPac® AS16 analytical column. The sample size was 2.0 ml, the flow rate was 1.0 ml/min, and the eluent was 35 mM sodium hydroxide. The amount of perchlorate adsorbed onto the anion-exchange resin was calculated by a mass balance relationship [28]. Langmuir adsorption isotherm was used to model the perchlorate adsorption behavior:

$$q_e = \frac{Q^0 b C_e}{1 + b C_e} \tag{1}$$

where q_e is the amount of adsorbed perchlorate on anion-exchange resin at equilibrium (mg/g), Q^0 the maximum adsorption capacity (mg/g), b a constant related to the affinity of the binding sites (*l*/mg), and C_e the perchlorate concentration in solution at equilibrium (mg/*l*).

To measure kinetic uptake of perchlorate onto the prepared materials, semi-batch adsorption experiments were performed. Sample powder of 0.1 g was mixed with 1 *l* of 0.1 mmol/*l* perchlorate aqueous solution. The suspended samples of 5 ml were taken at various time intervals under vigorous stirring of the solution. The samples were filtered with a 0.45 μm pore filter unit, and the perchlorate concentration of the filtrate was measured by using an IC system. Pseudo-second-order equation was used to model the kinetic data of perchlorate adsorption on the prepared anion-exchange resins [25,26,28]:

$$\frac{dq_t}{dt} = k_2 (q_e - q_t)^2 \tag{2}$$

where k_2 is the rate constant of pseudo-second-order adsorption (g/mg·min) and q_t the amount of adsorbed perchlorate on the anion-exchange resin at time t (mg/g). The integrated form of Eq. (2) is expressed as:

$$\frac{t}{q_t} = \frac{1}{k_2 q_e^2} + \frac{1}{q_e} t \tag{3}$$

RESULTS AND DISCUSSION

1. Characterization

N_2 adsorption-desorption isotherms of the prepared materials were determined at 77 K and shown in Fig. 1(a) and Fig. 2(a) for the MCM-type materials and SBA-type materials, respectively. All prepared materials showed type IV isotherm classified by IUPAC, which is typical of mesoporous materials [36]. In the adsorption-desorption isotherms of MCM-type materials, adsorption steps were observed in

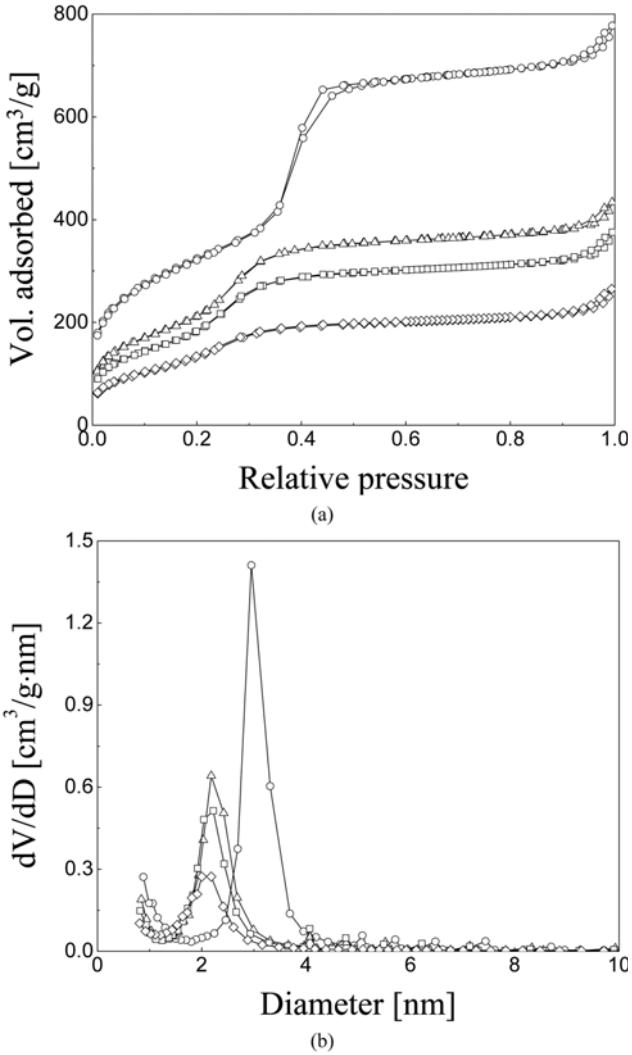

Fig. 1. (a) N_2 adsorption-desorption isotherms and (b) BJH pore size distributions of MCM-41 (○), M-1N (△), M-2N (□), and M-3N (◇).

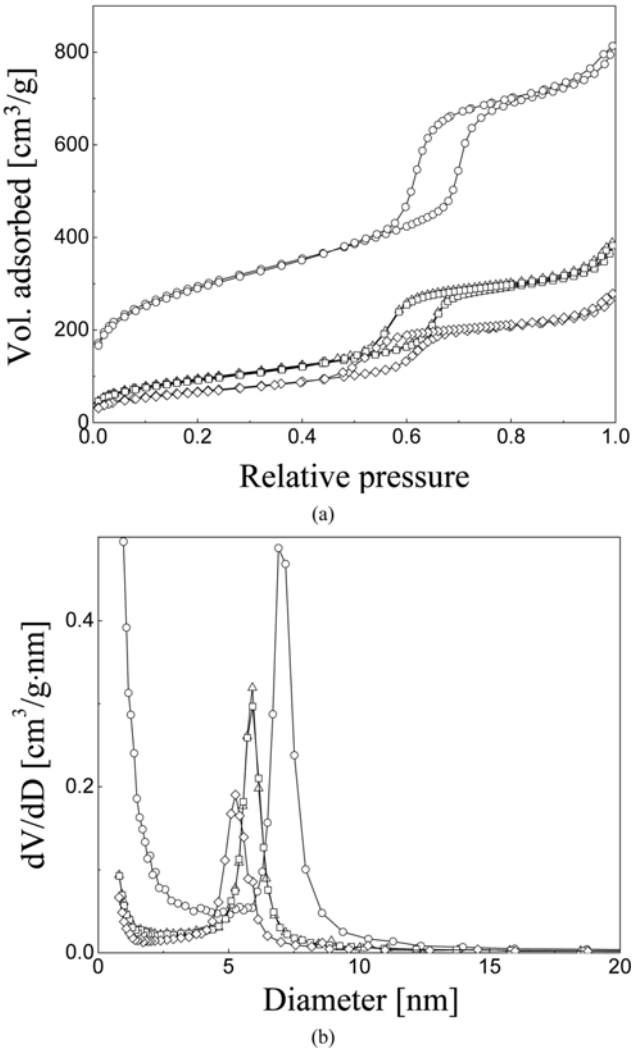

Fig. 2. (a) N_2 adsorption-desorption isotherms and (b) BJH pore size distributions of SBA-15 (○), S-1N (△), S-2N (□), and S-3N (◇).

Table 1. Properties of the prepared anion-exchange resins: surface area, pore diameter, pore volume, d spacing, relative intensities, and number of functional groups

Sample	Surface area[a] [m^2/g]	Pore diameter[b] [nm]	Pore volume[c] [cm^3/g]	d_{100} [nm]	Ligand[d] [mmol/g]	Ligand[e] [/nm^2]	Ligand[f] [/nm^2]
MCM-41	1168	3.0	1.14	3.85	-	-	-
M-1N	838	2.2	0.63	3.75	1.74	1.25	0.90
M-2N	746	2.2	0.53	3.75	0.98	0.79	0.51
M-3N	550	2.2	0.37	3.69	1.14	1.25	0.59
SBA-15	1029	6.9	1.20	10.14	-	-	-
S-1N	350	5.9	0.54	9.91	1.52	2.61	0.89
S-2N	342	5.9	0.54	9.91	0.79	1.39	0.46
S-3N	249	5.3	0.39	9.91	1.05	2.54	0.62

[a]BET surface area
[b]The most probable pore diameter in BJH adsorption pore size distribution
[c]Single point total pore volume
[d]Concentration of functional groups in the anion-exchange resins
[e]Number density of functional groups based on the surface area of each anion-exchange resin
[f]Number density of functional groups based on the bare mesoporous materials

the range less than 0.5 of relative pressure. The step was reversible for all the MCM-type materials, and became less marked when the length of functional groups increased. No hysteresis loop from framework mesopores was observed in the nitrogen desorption curve. This indicates that the cylindrical mesopore diameter is less than 4 nm, and that the pore size distribution is uniform [37]. SBA-type materials had adsorption steps in the range larger than 0.5 of P/P_0 values showing hysteresis curves. These isotherm curves show the typical characteristics of MCM-41 and SBA-15 materials. Both MCM-type and SBA-type materials had narrow and homogeneous pore size distributions even after the functionalization of chelating ligands as shown in Fig. 1(b) and Fig. 2(b).

Table 1 summarizes the textural properties and pore characteristics of the prepared materials. The bare mesoporous silica materials, MCM-41 and SBA-15, showed large surface areas of 1,168 and 1,029 m^2/g, respectively. After impregnating the amine ligands (M-1N, M-2N, M-3N, S-1N, S-2N, and S-3N), the surface areas, pore sizes, and pore volumes decreased logically due to the incorporation of organic groups onto the mesopores. As expected, functionalization induced a clear decrease of the framework mesopore sizes of the functionalized MCM materials and SBA materials, and of the corresponding mesoporous volumes. This finding is consistent with the general observation that the surface areas of the mesoporous silica materials prepared by surface functionalization decrease with the size and amount of the chelating ligands [12]. However, all MCM-type and SBA-type materials still exhibited mono-disperse pore size distributions and comparable mesopore accessibili-

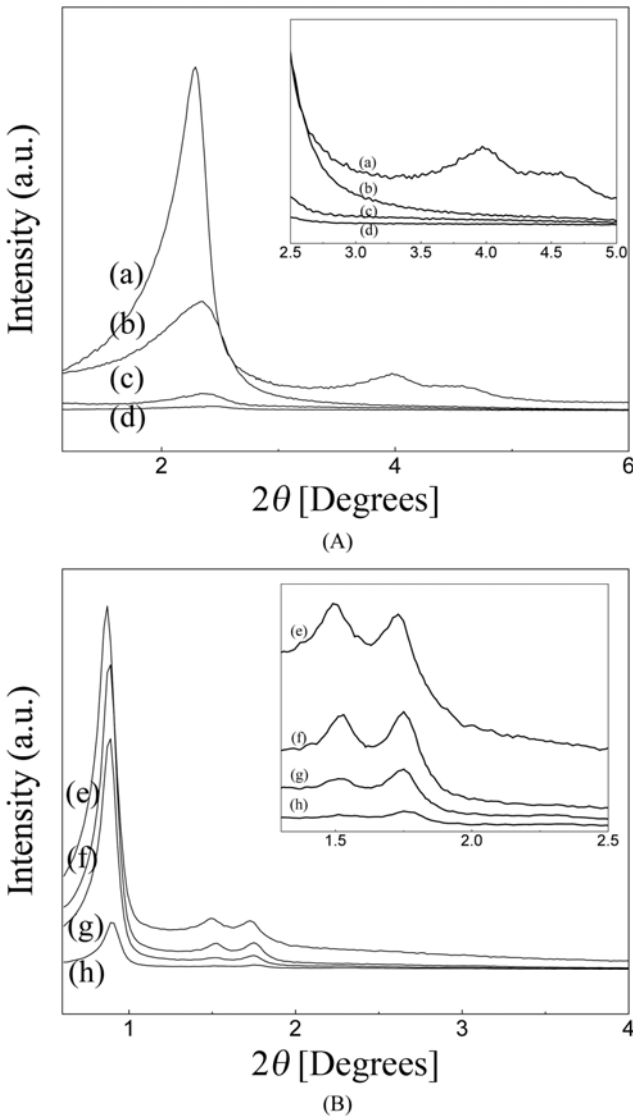

Fig. 3. XRD patterns of MCM-41 (a), M-1N (b), M-2N (c), M-3N (d), SBA-15 (e), S-1N (f), S-2N (g), and S-3N (h).

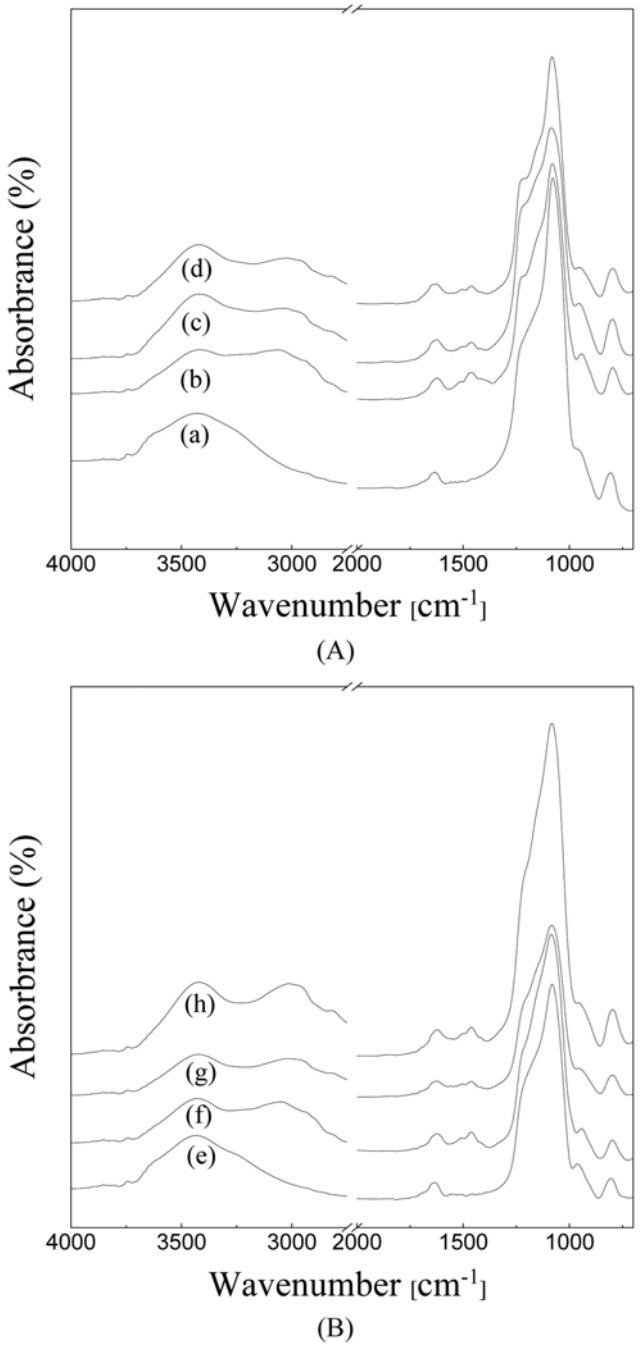

Fig. 4. FTIR spectra of MCM-41 (a), M-1N (b), M-2N (c), M-3N (d), SBA-15 (e), S-1N (f), S-2N (g), and S-3N (h): The sprctra (b), (c), (d), (f), (g), and (h) were shifted vertically 50%, 50%, 80%, 10%, 30%, and 50% up respectively for clarity.

ties even after the surface functionalization procedure.

XRD patterns of the prepared materials were obtained and shown in Fig. 3. XRD patterns indicate that MCM-41 and SBA-15 have typical hexagonal structures showing one main reflection and two additional weak reflections corresponding to the (100), (110), and (200) diffraction planes respectively [36]. Compared with the XRD spectrum of MCM-41, amine-functionalized materials showed rather broad reflections with lower intensities of the corresponding peak in the order of M-1N>M-2N>M-3N and the weak reflections disappeared (inset of Fig. 3A), showing the decrease of the crystallinity due to the functionalization. The structure orderness decreased with the length of amine ligands. SBA-15 type anion-exchange resins also showed decreased intensities of the corresponding peaks in the order of S-1N>S-2N>S-3N, showing also the decreased structural orderness with the length of amine ligands. While the weak reflections disappeared in MCM-41 type anion-exchange resins, S-1N, S-2N, and S-3N still had the second and third reflections, indicating that the amine-functionalized SBA-15 materials still had the clear hexagonal structures. This might be ascribed to the higher wall thickness value of SBA-15 than that of MCM-41 material, thus resulting in the higher stability for the post-treatment process of the materials.

Fig. 4 shows the FTIR spectra of the prepared materials. The absorption band of the surface silanol group of the hydrogen bonded type is observed at 3,200-3,600 cm^{-1} in all the prepared materials [29]. After the functionalization of chelating ligands, the intensity of the IR bands near 2,900 cm^{-1} arises from the -CH_2- stretching vibrations of the amine ligands [38]. The bands at 1,080 cm^{-1} are attributed to Si-O stretching from the siloxane bonds. Amine-functionalized anion-exchange resins (M-1N, M-2N, M-3N, S-1N, S-2N, and S-3N) have extra bands at 1,456 cm^{-1}, while MCM-41 and SBA-15 show no band at the same position. These bands confirm the presence of amine ligands in the samples, indicating the successful impregnation of functional groups [28,39].

The results of elemental analyses are shown in Table 1. In the bare mesoporous materials (MCM-41 and SBA-15), nitrogen was not detected indicating that there were no functional groups in MCM-41 and SBA-15. Considering all functional groups were located on the surface of the mesoporous silicas, the number of functional groups on the unit surface area was calculated using the results of elemental analyses and BET surface areas of each sample (Table 1). In the previous studies [26,28,40], the surface densities of functional groups, such as quaternary ammoniums or thiols, ranged from 0.1 to 2.4 nm^{-2}. All the anion-exchange resins prepared in this work had comparable surface densities of functional groups ranging from 0.79 to 2.61 nm^{-2} (7^{th} column of Table 1). SBA-type anion-exchange resins had relatively larger densities of functional groups, showing approximately twice the values of those of MCM-type materials due to the smaller surface areas of SBA-type anion-exchange resins. Because the syntheses of anion-exchange resins were carried out via impregnation method, the number densities of the functional groups were also obtained on the basis of the surface area of the bare mesoporous silica. The calculated ligand densities ranged from 0.46 to 0.90 nm^{-2} (8^{th} column of Table 1). In this case, the number densities of surface functional groups in MCM-type mesoporous materials showed similar values with those of SBA-type materials, indicating that the amine groups were successfully functionalized on the surface of mesoporous materials.

2. Anion Adsorption

Equilibrium adsorption experiments of perchlorate anions were carried out in single-solute solutions using the prepared anion-exchange resins. MCM-41 and SBA-15 with no functional groups showed little adsorption capabilities for perchlorate anions with adsorption capacities less than 25 mg/g in the experimental concentrations. Compared with the bare mesoporous silicas, the prepared anion-exchange resins showed larger adsorption capacities for perchlorate anions, indicating that amine functional groups incorporated onto the pore surfaces had a strong affinity for perchlorate anions. As shown in Table 2 and Fig. 5, the equilibrium adsorption isotherms were well fitted with the Langmuir isotherm model, showing the R^2 values over 0.94 for all the prepared anion-exchange resins. Perchlorate adsorption capacities obtained from the Langmuir model were 120.5, 163.9, 175.4, 142.9, 99.1, and 114.9 mg/g for M-1N, M-2N, M-3N, S-1N, S-2N, and S-3N, respectively. Perchlorate adsorption capacities of M-2N (163.9 mg/g) and M-3N (175.4 mg/g) were larger than the maximum adsorption capacity of 142.9 mg/g among the previous researches, showing the excellence of the prepared anion-exchange resins in this work [26-28]. The normalized adsorption capacities, Q_{NA}, of perchlorate per unit surface area and per unit functional groups were determined using BET surface areas, concentrations of functional groups, and maximum adsorption capacities obtained from the Langmuir isotherm (Table 2). SBA-type anion-exchange resins had relatively larger Q_{NA} values ranging from 0.29 to 0.46 mg/m^2 due to the smaller surface areas and larger surface

Table 2. Langmuir isotherm parameters in the adsorption of perchlorate on the prepared anion-exchange resins

Sample	Q^0 [mg/g]	b [L/mg]	R^2	Q_{NA} [mg/m^2]	Q_{NA} [mg/mmol]	ClO_4^-/ligand
M-1N	120.5	1.49×10^{-3}	0.9568	0.14	69.3	0.70
M-2N	163.9	1.36×10^{-3}	0.9444	0.22	167.2	1.68
M-3N	175.4	1.83×10^{-3}	0.9502	0.32	153.9	1.55
S-1N	142.9	1.48×10^{-3}	0.9775	0.41	94.0	0.95
S-2N	99.1	0.98×10^{-3}	0.9778	0.29	125.4	1.26
S-3N	114.9	1.99×10^{-3}	0.9579	0.46	109.4	1.10

Q^0: Maximum adsorption capacity

b: Langmuir constant

R^2: Correlation coefficient

Q_{NA}: Normalized adsorption capacity per unit surface area or unit amount of ligands

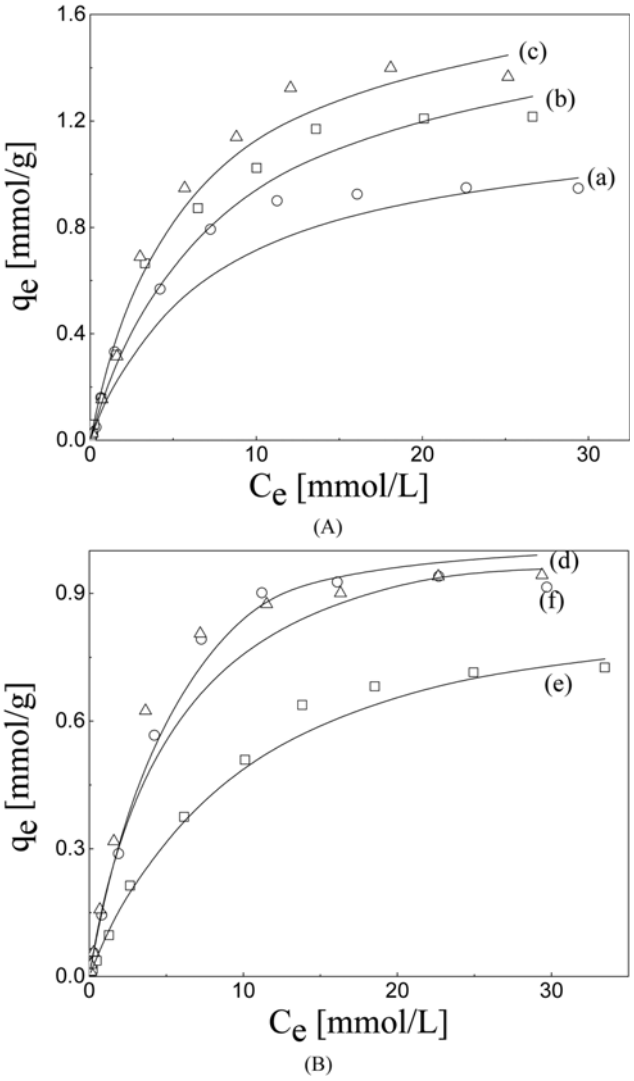

Fig. 5. Adsorption isotherms of perchlorate on M-1N (a), M-2N (b), M-3N (c), S-1N (d), S-2N (e), and S-3N (f): Data were fitted with Langmuir model (solid lines).

concentrations of functional groups than those of MCM-type materials ranging from 0.14 to 0.32 mg/m^2. For the same reasons, MCM-type anion-exchange resins showed larger Q_{NA} values per unit functional groups, ranging from 69.3 to 167.2 mg/mmol than those values of SBA-type materials ranging from 94.0 to 125.4 mg/mmol. The ratios of the amount of the adsorbed perchlorate anions to the amount of surface functional groups were also obtained from the equilibrium isotherm data. The ClO_4^-/ligand ratio values of MCM-type anion-exchange resins were rather higher than those of SBA-type materials, implying that MCM-type anion-exchange resins had higher adsorption efficiencies than SBA-type materials, as shown in the larger adsorption capacities of MCM-type materials in Table 2. This might be ascribed to the smaller pore size of MCM-type materials, which decreased the distance of the functional ligands across the mesopores resulting in the collaborative chelating activities of the functional groups across the mesopores.

To determine the kinetic adsorption rate, perchlorate anion adsorption experiments were performed using a semi-batch reactor

Table 3. Adsorption kinetic parameters calculated from pseudo-second-order kinetic model

Sample	$q_{e,exp}$ [mg/g]	$q_{e,cal}$ [mg/g]	k_2 [g/mg·min]	R^2
M-1N	39.2	39.2	2.06	0.9996
M-2N	49.8	50.0	1.04	0.9984
M-3N	36.9	37.0	0.79	0.9981
S-1N	34.0	33.9	0.64	0.9973
S-2N	42.5	42.5	0.93	0.9982
S-3N	51.2	51.3	0.87	0.9985

$q_{e,exp}$: Adsorption capacity measured from experiment
$q_{e,cal}$: Adsorption capacity estimated by the kinetic model
k_2: Rate constant of pseudo-second-order equation

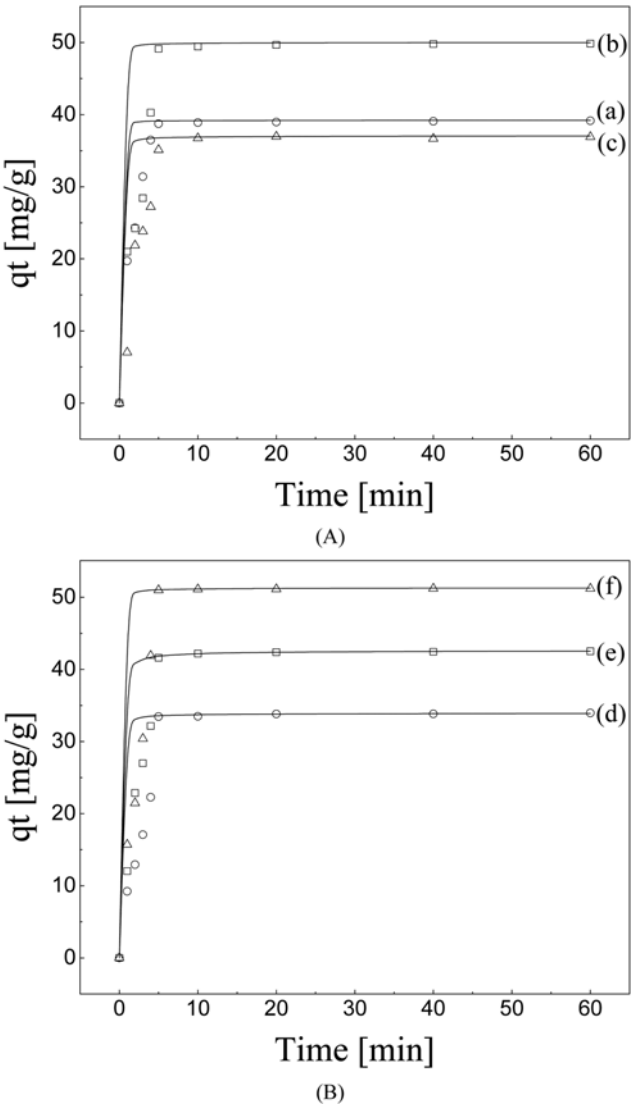

Fig. 6. Time-resolved uptake of perchlorate on M-1N (a), M-2N (b), M-3N (c), S-1N (d), S-2N (e), and S-3N (f), and fitting plots of the perchlorate adsorption kinetics which were obtained using pseudo-second-order kinetic model (solid lines).

(Table 3 and Fig. 6). The prepared anion-exchange resins showed fast adsorption rates for perchlorate. The required contact time to

reach equilibrium was less than 10 min for all the anion-exchange resins used. These results indicate that the contact time of 6 h was enough for the equilibrium adsorption experiments described in the above section. Adsorption kinetic data were fitted with a pseudo-second-order model because it was reported that the pseudo-second-order model showed best correlations with the experimental data in metal adsorption among the kinetic models, including pseudo-first-order model, pseudo-second-order model, and parabolic diffusion model [26]. The fitting plots and the parameters for the model were determined and shown in Fig. 6 and Table 3. The R^2 values for this kinetic model were larger than 0.99 for all the anion-exchange resins used, showing that the adsorption kinetic for the prepared anion-exchange resins followed well the pseudo-second-order model. The adsorption capacity estimated by the kinetic model, $q_{e,cal}$ also coincided well with the experimental data, $q_{e,exp}$ (Table 3). The $q_{e,cal}$ values were smaller than those of the Q^0 values obtained from adsorption isotherms, showing the values from 21% to 45% of the Q^0 values. Generally, the adsorption capacity calculated using pseudo-second-order equation from kinetic data shows smaller value than the adsorption capacity obtained from Langmuir model, which shows the maximum adsorption capacity [27].

CONCLUSIONS

We synthesized amine-functionalized mesoporous anion-exchange resins and used them for the removal of perchlorate anions from aqueous solutions. The prepared anion-exchange resins showed high perchlorate adsorption capacity of 175.4 mg/g (M-3N). This value is much larger than those of anion-exchange resins for perchlorate or perrhenate anions in the previous studies. The large adsorption capacity might be ascribed to the well developed mesoporous structures of the prepared materials. Among the prepared materials, MCM-type adsorbents showed higher adsorption capacities than SBA-type adsorbents. This might be due to the difference of pore structures between the two materials used. The prepared anion-exchange resins also showed fast adsorption kinetic performances. These results show that the prepared anion-exchange resins can be an effective alternative for the removal of perchlorate anions from water.

ACKNOWLEDGEMENT

This research was supported by Basic Science Research Program through the National Research Foundation of Korean (NRF) funded by the Ministry of Education, Science and Technology (2010-0007569).

REFERENCES

1. R. J. Bull, A. C. Chang, C. F. Cranor, R. C. Shank and R. Trussell, *Perchlorate in drinking water: A science and policy review*, Urban Water Research Center, University of California, Irvine, CA (2004).
2. G. M. Brown and B. Gu, in *Perchlorate: Environmental occurrence, interactions and treatment*, B. Gu and J. D. Coates Eds., Springer, New York (2006).
3. Yonhap News, July 28 (2006).
4. B. E. Logan, *Environ. Sci. Technol.*, **35**(23), 482A (2001).
5. Z. Xiong, D. Zhao and W. F. Harper, *Ind. Eng. Chem. Res.*, **46**(26), 9213 (2007).
6. K. Hristovski, P. Westerhoff, T. Moller, P. Sylvester, W. Condit and H. Mash, *J. Hazard. Mater.*, **152**(1), 397 (2008).
7. I. H. Yoon, X. G. Meng, C. Wang, K. W. Kim, S. Bang, E. Choe and L. Lippincott, *J. Hazard. Mater.*, **164**(1), 87 (2009).
8. B. Gu, Y.-K. Ku and G. M. Brown, *Federal Facilities Environ. J.*, Spring, 75 (2003).
9. B. Gu, Y.-K. Ku and G. M. Brown, *Environ. Sci. Technol.*, **39**(3), 901 (2005).
10. B. Gu, G. M. Brown and C.-C. Chiang, *Environ. Sci. Technol.*, **41**(17), 6277 (2007).
11. Y. H. Ju, O. F. Webb, S. Dai, J. S. Lin and C. E. Barnes, *Ind. Eng. Chem. Res.*, **39**(2), 550 (2000).
12. B. Lee, L. L. Bao, H. J. Im, S. Dai, E. W. Hagaman and J. S. Lin, *Langmuir*, **19**(10), 4246 (2003).
13. S. Zhang, Y. Shao, J. Liu, I. A. Aksay and Y. Lin, *ACS Appl. Mater. Interfaces*, **3**(9), 3633 (2011).
14. C. T. Kresge, M. E. Leonowicz, W. J. Roth, J. C. Vartuli and J. S. Beck, *Nature*, **359**(6397), 710 (1992).
15. P. T. Tanev and T. J. Pinnavaia, *Science*, **267**(5199), 865 (1995).
16. D. Y. Zhao, J. L. Feng, Q. S. Huo, N. Melosh, G. H. Fredrickson, B. F. Chmelka and G. D. Stucky, *Science*, **279**(5350), 548 (1998).
17. A. Walcarius and L. Mercier, *J. Mater. Chem.*, **20**, 4478 (2010).
18. H. Yoshitake, T. Yokoi and T. Tatsumi, *Chem. Mater.*, **14**(11), 4603 (2002).
19. G. E. Fryxell, J. Liu, T. A. Hauser, Z. M. Nie, K. F. Ferris, S. Mattigod, M. L. Gong and R. T. Hallen, *Chem. Mater.*, **11**(8), 2148 (1999).
20. Y. H. Lin, G. E. Fryxell, H. Wu and M. Engelhard, *Environ. Sci. Technol.*, **35**(19), 3962 (2001).
21. H. Yoshitake, T. Yokoi and T. Tatsumi, *Chem. Mater.*, **15**(8), 1713 (2003).
22. M. Jang, E. W. Shin, J. K. Park and S. I. Choi, *Environ. Sci. Technol.*, **37**(21), 5062 (2003).
23. E. W. Shin, J. S. Han, M. Jang, S. H. Min, J. K. Park and R. M. Rowell, *Environ. Sci. Technol.*, **38**(3), 912 (2004).
24. Y. H. Kim, C. M. Kim, I. H. Choi, S. Rengaraj and J. H. Yi, *Environ. Sci. Technol.*, **38**(3), 924 (2004).
25. T. H. Kim, M. Jang and J. K. Park, *Micropor. Mesopor. Mat.*, **108** (1-3), 22 (2008).
26. B. Lee, Y.-S. Chung and C. Park, *Korean Chem. Eng. Res.*, **46**(2), 436 (2008).
27. Y.-S. Chung, B. Lee, K.-H. Choo and S.-J. Choi, *J. Ind. Eng. Chem.*, **17**(1), 114 (2011).
28. S. D. Lee, B. Lee and K.-H. Choo, *Korean J. Chem. Eng.*, **28**(6), 1393 (2011).
29. B. Lee, Y. Kim, H. Lee and J. Yi, *Micropor. Mesopor. Mater.*, **50**(1), 77 (2001).
30. Z. Bacsik, N. Ahlsten, A. Ziadi, G. Zhao, A. E. Garcia-Bennett, B. Martín-Matute and N. Hedin, *Langmuir*, **27**(17), 11118 (2011).
31. A. Heydari-Gorji, Y. Yang and A. Sayari, *Energy Fuels*, **25**(9), 4206 (2011).
32. B. Lee, Z. Ma, Z. T. Zhang, C. Park and S. Dai, *Micropor. Mesopor. Mater.*, **122**(1-3), 160 (2009).
33. H. Zheng, Y. Wang and S. Che, *J. Phys. Chem. C*, **115**(34), 16803 (2011).
34. J. S. Beck, J. C. Vartuli, W. J. Roth, M. E. Leonowicz, C. T. Kresge, K. D. Schmitt, C. T. W. Chu, D. H. Olson, E. W. Sheppard, S. B.

Mccullen, J. B. Higgins and J. L. Schlenker, *J. Am. Chem. Soc.*, **114** (27), 10834 (1992).
35. D. Y. Zhao, Q. S. Huo, J. L. Feng, B. F. Chmelka and G. D. Stucky, *J. Am. Chem. Soc.*, **120**(24), 6024 (1998).
36. Y. H. Kim, B. Lee, K. H. Choo and S. J. Choi, *Micropor. Mesopor. Mater.*, **138**(1-3), 184 (2011).
37. F. Rouquerol, G. Rouquerol and K. Sing, *Adsorption by powders and porous solids*, Academic Press (1999).
38. B. Lee, H. J. Im, H. M. Luo, E. W. Hagaman and S. Dai, *Langmuir*, **21**(12), 5372 (2005).
39. G. Socrates, *Infrared and raman characteristic group frequencies*, 3rd Ed., Wiley, Chichester (2001).
40. Y. Kim, B. Lee, Y. S. Cho and J. Yi, *Korean Chem. Eng. Res.*, **39**(2), 228 (2001).